

Control of the Transition Temperatures of Metallomesogens by Specific Interface Design: Application to Mn₁₂ Single Molecule Magnets.

Emmanuel Terazzi^[a], Thomas Binderup Jensen^[a], Bertrand Donnio^[b], Kerry-Lee Buchwalder^[a], Cyril Bourgogne^[b], Guillaume Rogez^[b], Benoît Heinrich^[b], Jean-Louis Gallani^[b], and Claude Piguet^[a]

^[a] Department of Inorganic, Analytical and Applied Chemistry, University of Geneva, 30 quai E. Ansermet, CH-1211 Geneva 4 (Switzerland)

E-mails: Emmanuel.Terazzi@unige.ch

^[b] Institut de Physique et Chimie des Matériaux de Strasbourg (IPCMS), UMR 7504 (CNRS-Université de Strasbourg), 23 rue du Loess, BP43, 67034, Strasbourg cedex 2, France.

Supporting Information

(12 pages)

General: Chemicals were purchased from Acros, Alfa Aesar and Aldrich, and used without further purification unless otherwise stated. Silicagel plates Merck 60 F₂₅₄ were used for thin layer chromatography (TLC) and Fluka silica gel 60 (0.04-0.063 mm) was used for preparative column chromatography.

Preparation of clusters [Mn₁₂O₁₂(Li-H)₁₆(H₂O)₄] (i = 4, 5): To a suspension of [Mn₁₂O₁₂(CH₃CO₂)₁₆(H₂O)₄] (0.10 g, 1 eq.) in 20 mL of CH₂Cl₂/toluene (1:1), Li (*i* = 4 or 5; 32 eq.) was added. The mixture was heated at 45 °C under stirring for 24 h. A black solution was obtained. The solution was filtered and concentrated. CH₂Cl₂/toluene (40 mL) was added and then evaporated. This procedure was repeated four times for completely removing acetic acid. Samples of about 0.20 g of the resulting brown mixtures were used for purification by two successive size exclusion SX-1 Bio-Beads (CH₂Cl₂) column chromatography. The products were dried for 24 h under vacuum at 60 °C. [Mn₁₂O₁₂(Li-H)₁₆(H₂O)₄] (*i* = 4, 5) were obtained as brown solids in 80 % yield.

Spectroscopic and Analytical Measurements. ¹H and ¹³C NMR spectra were recorded at 298 K on *Bruker Avance* 400 MHz spectrometer. Chemical shifts are given in ppm with respect to TMS. Elemental analyses were performed by Dr. H. Eder from the Microchemical Laboratory of the University of Geneva. TGA was performed with a Seiko TG/DTA 320 thermogravimetric balance (under N₂). DSC traces were obtained with a Mettler Toledo DSC1 Star Systems differential scanning calorimeter from 3 to 5 mg samples (5°C min⁻¹, under N₂). Characterizations of the mesophases were performed with a Leitz Orthoplan Pol polarizing microscope with a Leitz LL 20×/0.40 polarizing objective and equipped with a Linkam THMS 600 variable temperature stage. The SAXS and WAXS patterns were obtained with three different experimental setups (I, II, III). In all cases, a linear monochromatic Cu-Kα1 beam ($\lambda = 1.5405\text{\AA}$) was obtained using a sealed-tube generator (900W) equipped with a bent quartz monochromator. In the first setup, the transmission Guinier geometry (I) was used, whereas Debye-Scherrer-like (II) and “flat film” (III) geometries were used in the second and third experimental set-ups respectively. In all cases, the crude product

was placed in a sealed cell (ca 20 mg). In setup I, diffraction patterns are recorded on an image plate and the sample temperature is controlled to within ± 0.3 °C in the 20 to 350 °C temperature range (for periodicities up to 80Å). In setup II, diffraction patterns are recorded with a curved Inel CPS120 counter gas-filled detector linked to a data acquisition computer (for periodicities up to 60Å) or on image plates (for periodicities up to 100Å); the sample temperature is controlled to within ± 0.05 °C in the 20 to 200 °C temperature range. In setup III, diffraction patterns (III) are recorded with a Inel LPS50 counter gas-filled detector linked to a data acquisition computer or on image plate (for periodicities up to 350Å), and the sample temperature controlled to within ± 0.01 °C in the 20 to 200 °C temperature range. In each case, exposure times were varied from 1 to 24h. The magnetic characterization of the sample was performed with a SQUID magnetometer (Quantum Design, MPMS XL) at temperatures between 1.8K and 400K. The applied field can reach a maximum value of 5 teslas. The sample was sonfined in a small gelatin capsule, which was inserted into the SQUID chamber by means of a plastic straw. Preliminary measurements confirmed the purely diamagnetic behaviour of the capsule and straw. The molecular modelling studies were performed on SGI Origin 2800 and Octane 2 calculators using Insight II and Discover 3 software from Accelrys (www.accelrys.com) with the esff forcefield. Energy minimisation of the model in a fixed cell was conducted down to a gradient of 1 kcal/mol, and was then equilibrated at 393 K by a 150 ps isothermal MD simulation (NVT-PBC ensemble, “velocity scaling” temperature control method, and a time step of 1 fs).

Table S1 Elemental Analysis for clusters $[\text{Mn}_{12}\text{O}_{12}(\text{Li-H})_{16}(\text{H}_2\text{O})_4]$ ($i = 4, 5$).

Compound	%C	%H	%N	%C	%H	%N
	found	found	found	calcd	calcd	calcd
$[\text{Mn}_{12}\text{O}_{12}(\text{L4-H})_{16}(\text{H}_2\text{O})_4] \cdot 11.7 \text{ H}_2\text{O}$	70.53	6.13	1.78	70.53	6.17	1.77
$[\text{Mn}_{12}\text{O}_{12}(\text{L5-H})_{16}(\text{H}_2\text{O})_4] \cdot 10.8 \text{ H}_2\text{O}$	70.85	6.42	1.75	70.84	6.31	1.74

Table S2 Indexation at a given temperature for the reflections detected in the liquid-crystalline phases by SA-XRD for clusters $[\text{Mn}_{12}\text{O}_{12}(\text{Li-H})_{16}(\text{H}_2\text{O})_4]$ ($i = 4, 5$). The values are given on second heating.

$T / ^\circ\text{C}$	$d_{hkl \text{ (mes)}} / \text{\AA}$	$I / \text{a.u.}$	$00l$	$d_{hkl \text{ (calc)}} / \text{\AA}$	
130°C	87.7	VS(Sh)	001	87.5	$d = 87.5 \text{ \AA}$
$[\text{Mn}_{12}\text{O}_{12}(\text{L4-H})_{16}(\text{H}_2\text{O})_4]$	43.6	VS(Sh)	002	43.7	$d' = 22.7 \text{ \AA}$
	22.7	VS(Br)	d'	-	
	4.50	S(Br)	-	-	
130°C	87.0	VS(Sh)	001	86.8	$d = 86.8 \text{ \AA}$
$[\text{Mn}_{12}\text{O}_{12}(\text{L5-H})_{16}(\text{H}_2\text{O})_4]$	43.3	VS(Sh)	002	43.4	$d' = 23.3 \text{ \AA}$
	23.3	VS(Br)	d'	-	
	4.50	S(Br)	-	-	

$d_{hkl \text{ (mes)}}$ and $d_{hkl \text{ (calc)}}$ are the measured and calculated diffraction spacing ; d is the lattice parameter of the smectic phase ; d' is the mean distance between the disordered clusters inside the layers of the smectic A phase ; I corresponds to the intensity of the reflections (VS : very strong, S : strong ; br and sh stand for broad and sharp) ; The $d_{001 \text{ (calc)}}$ are calculated according the formula: $\langle d_{001} \rangle_{\text{(calc)}} = \frac{1}{2} (d_{001 \text{ (exp)}} + 2d_{002 \text{ (exp)}})$.

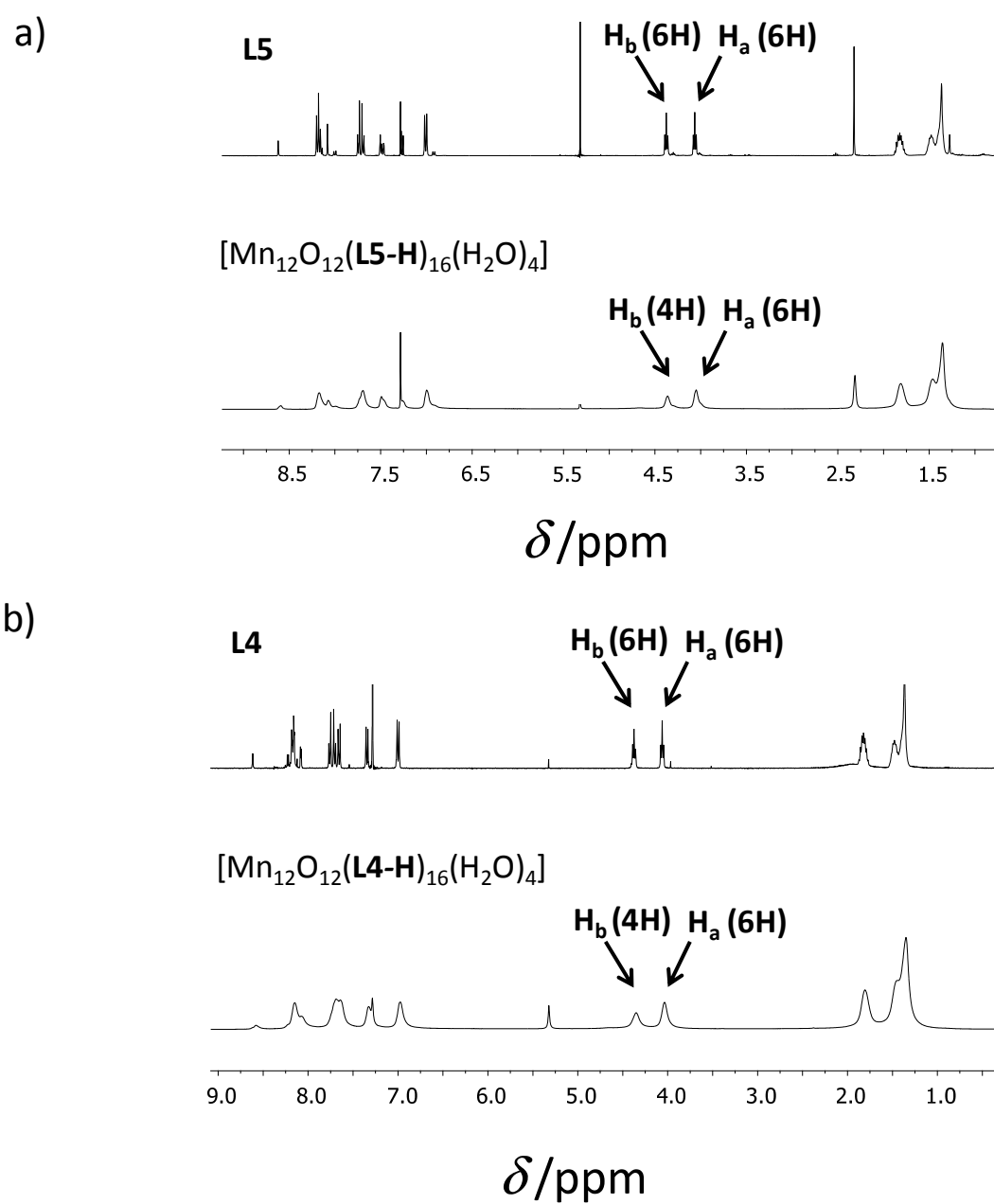
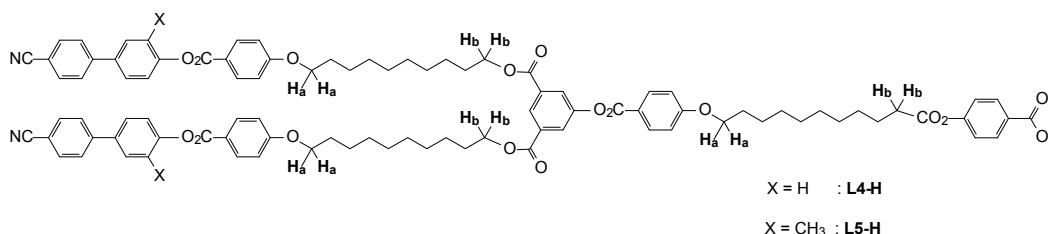


Fig. S1 (a) ¹H NMR of ligand **L5** (top) and cluster [Mn₁₂O₁₂(L5-H)₁₆(H₂O)₄] (down) (CDCl₃, 298 K) (b) (a) ¹H NMR of ligand **L4** (top) and cluster [Mn₁₂O₁₂(L4-H)₁₆(H₂O)₄] (down) (CDCl₃, 298 K).

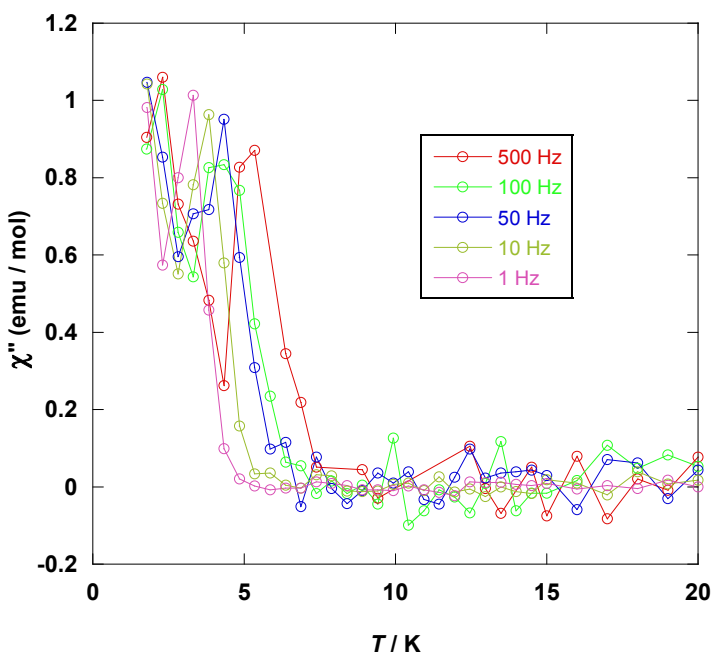


Fig. S2 Temperature dependence of χ'' for $[\text{Mn}_{12}\text{O}_{12}(\text{L5-H})_{16}(\text{H}_2\text{O})_4]$. χ'' is the imaginary components of the molar magnetic susceptibility at zero dc field with a field of 3.5 Oe oscillating at various frequencies.

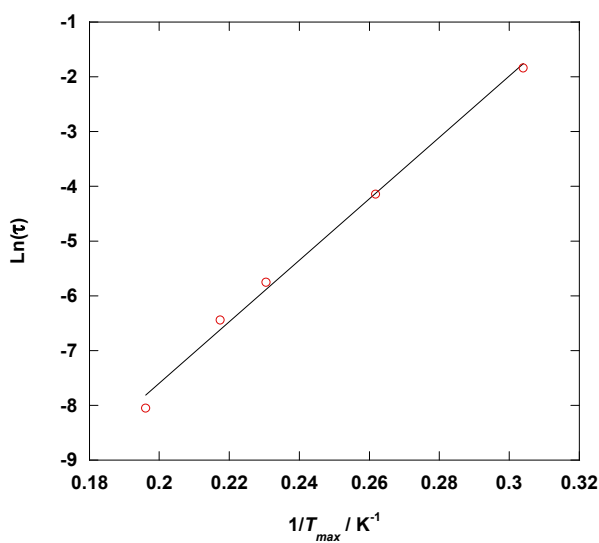


Fig. S3 Plot of the natural logarithm of relaxation rate, $\ln(\tau)$ versus the inverse of temperature for $[\text{Mn}_{12}\text{O}_{12}(\text{L5-H})_{16}(\text{H}_2\text{O})_4]$. Full line corresponds to best fit using an Arrhenius law (see text)

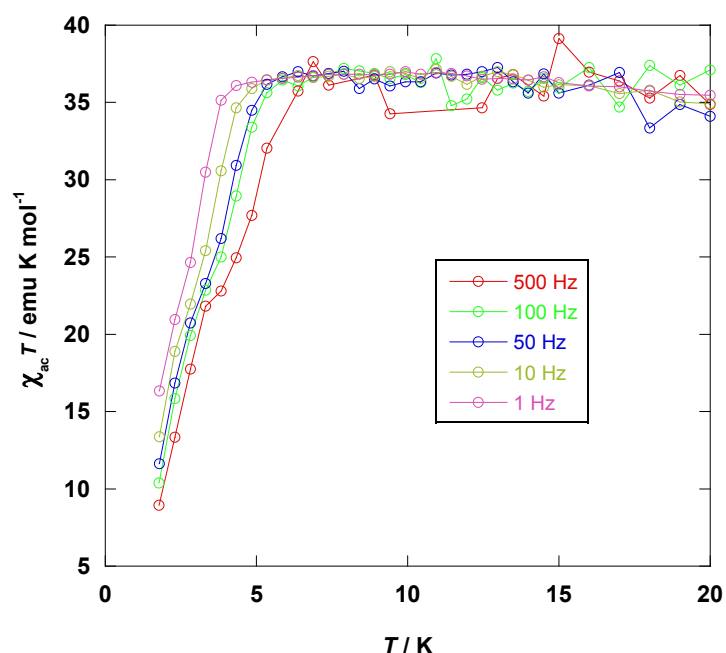


Fig. S4 Temperature dependence of $\chi_{ac}T$ for $[\text{Mn}_{12}\text{O}_{12}(\text{L5-H})_{16}(\text{H}_2\text{O})_4]$ ($\chi_{ac} = \sqrt{(\chi')^2 + (\chi'')^2}$).

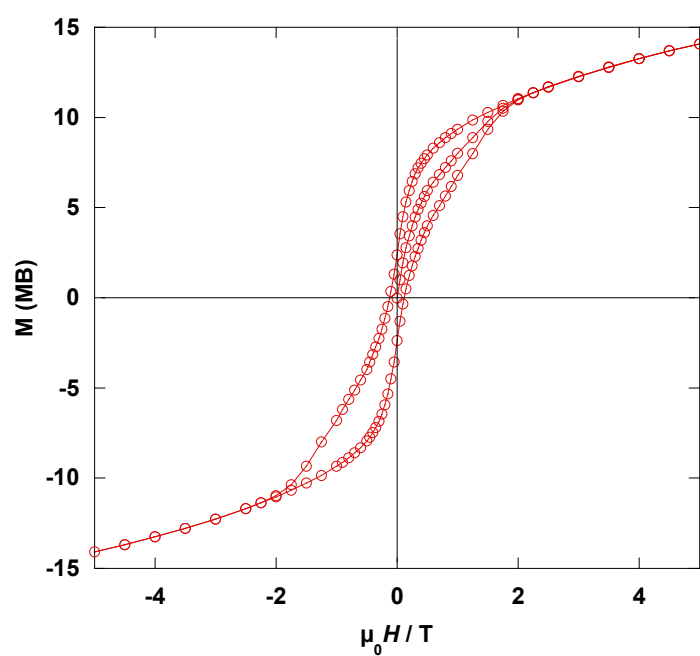


Fig. S5 Magnetization versus applied field for $[\text{Mn}_{12}\text{O}_{12}(\text{L5-H})_{16}(\text{H}_2\text{O})_4]$ at 1.8 K. Full line is just a guide for the eye.

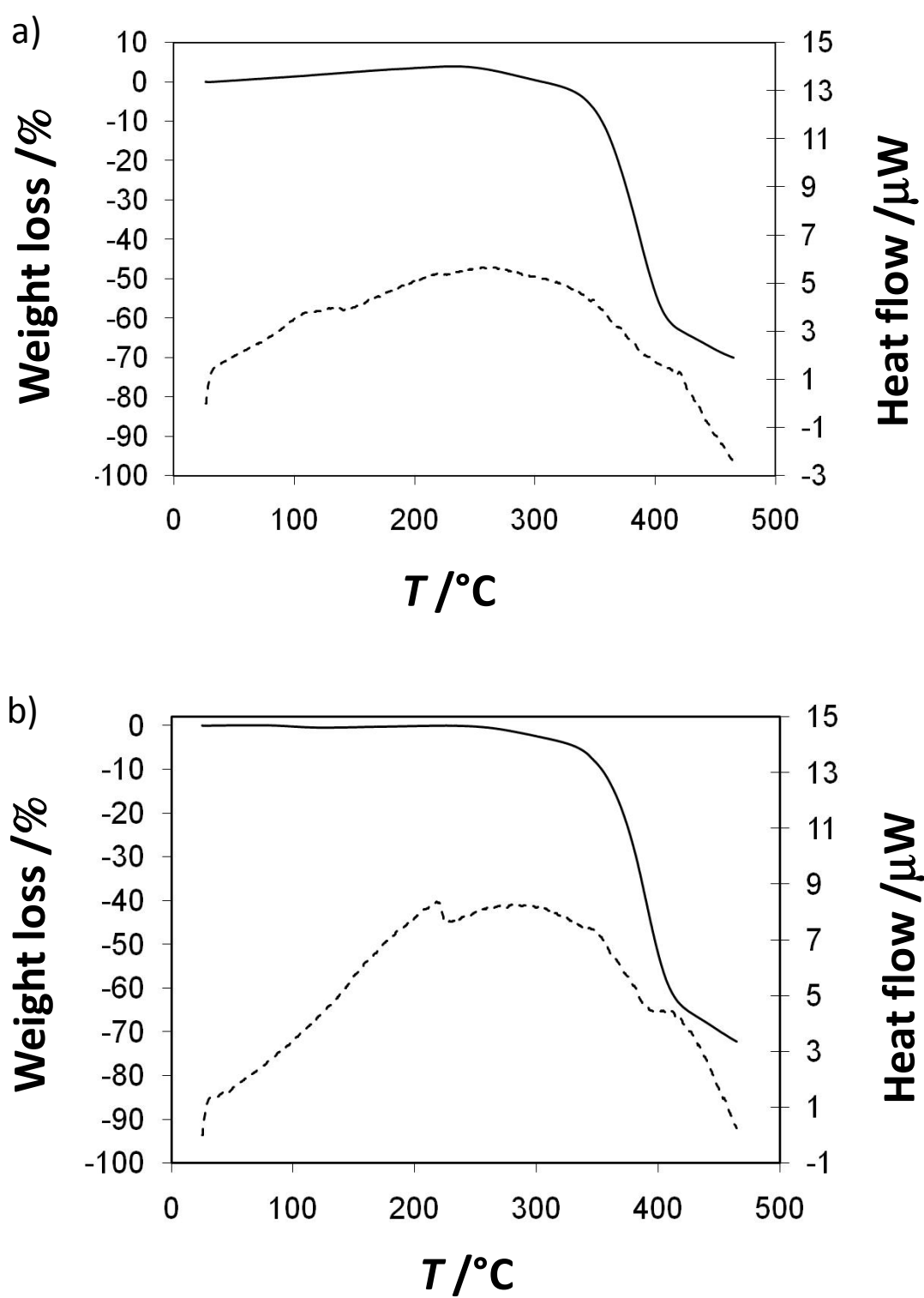


Fig. S6 (a) TGA of $[\text{Mn}_{12}\text{O}_{12}(\text{L5-H})_{16}(\text{H}_2\text{O})_4]$ at $5^\circ\text{C}/\text{min}$ (b) TGA of $[\text{Mn}_{12}\text{O}_{12}(\text{L4-H})_{16}(\text{H}_2\text{O})_4]$ at $5^\circ\text{C}/\text{min}$.

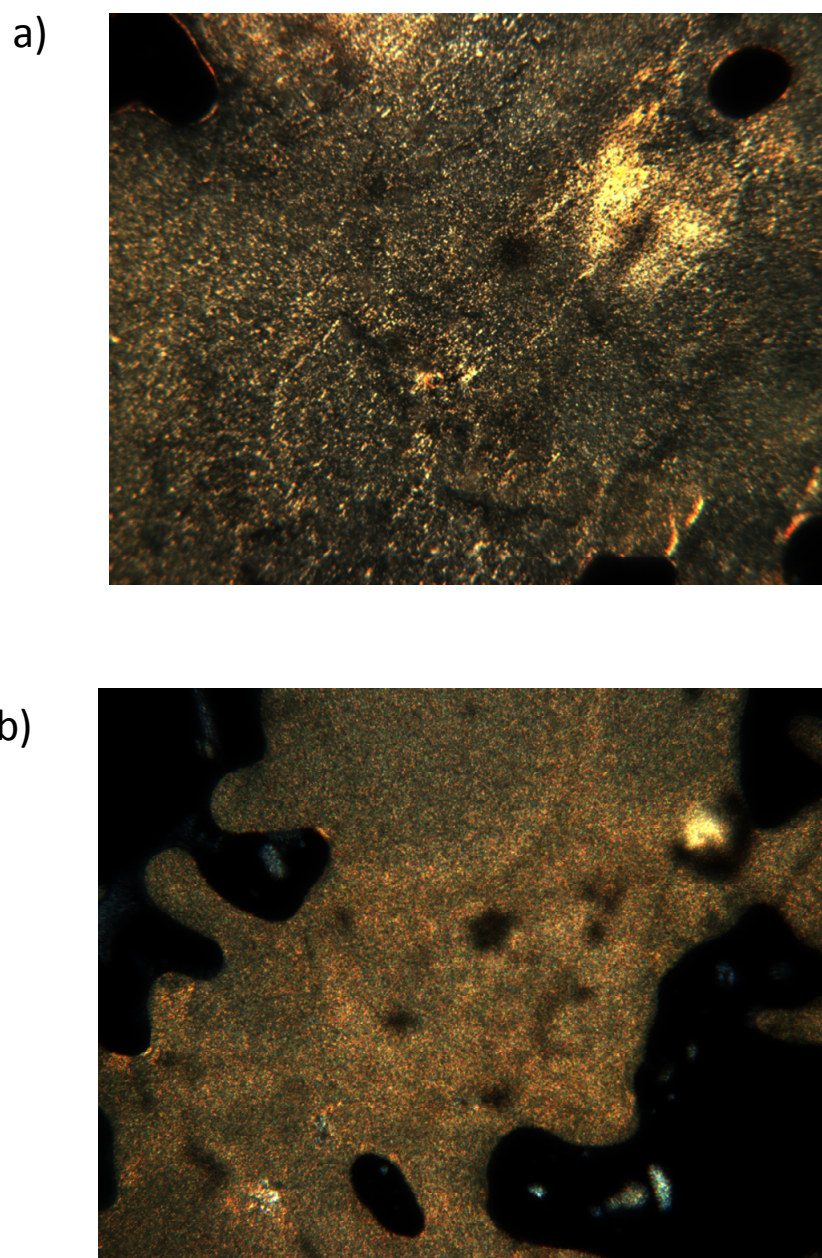


Fig. S7 (a) Optical textures observed by POM for cluster $[\text{Mn}_{12}\text{O}_{12}(\text{L5-H})_{16}(\text{H}_2\text{O})_4]$ in SmA mesophase at 130°C after cooling from is from the isotropic liquid (b) Optical textures observed by POM for cluster $[\text{Mn}_{12}\text{O}_{12}(\text{L4-H})_{16}(\text{H}_2\text{O})_4]$ in SmA mesophase at 190°C after cooling from is from the isotropic liquid.

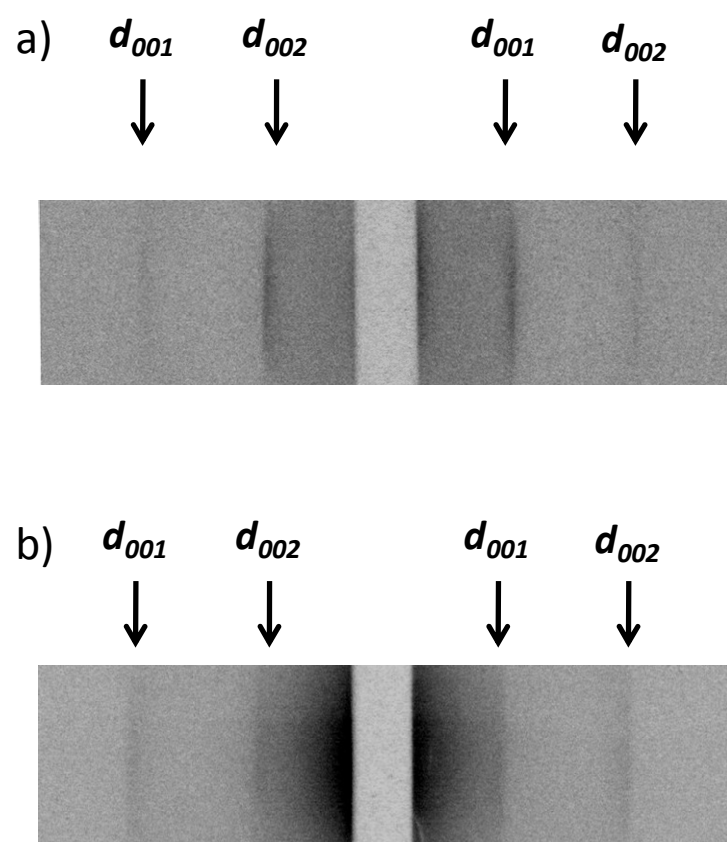


Fig. S8 (a) SAXS image plate of the SmA liquid crystalline phase of $[\text{Mn}_{12}\text{O}_{12}(\text{L5-H})_{16}(\text{H}_2\text{O})_4]$ (130°C) and indexation. (b) SAXS image plate of the SmA liquid crystalline phase of $[\text{Mn}_{12}\text{O}_{12}(\text{L4-H})_{16}(\text{H}_2\text{O})_4]$ (130°C) and indexation.

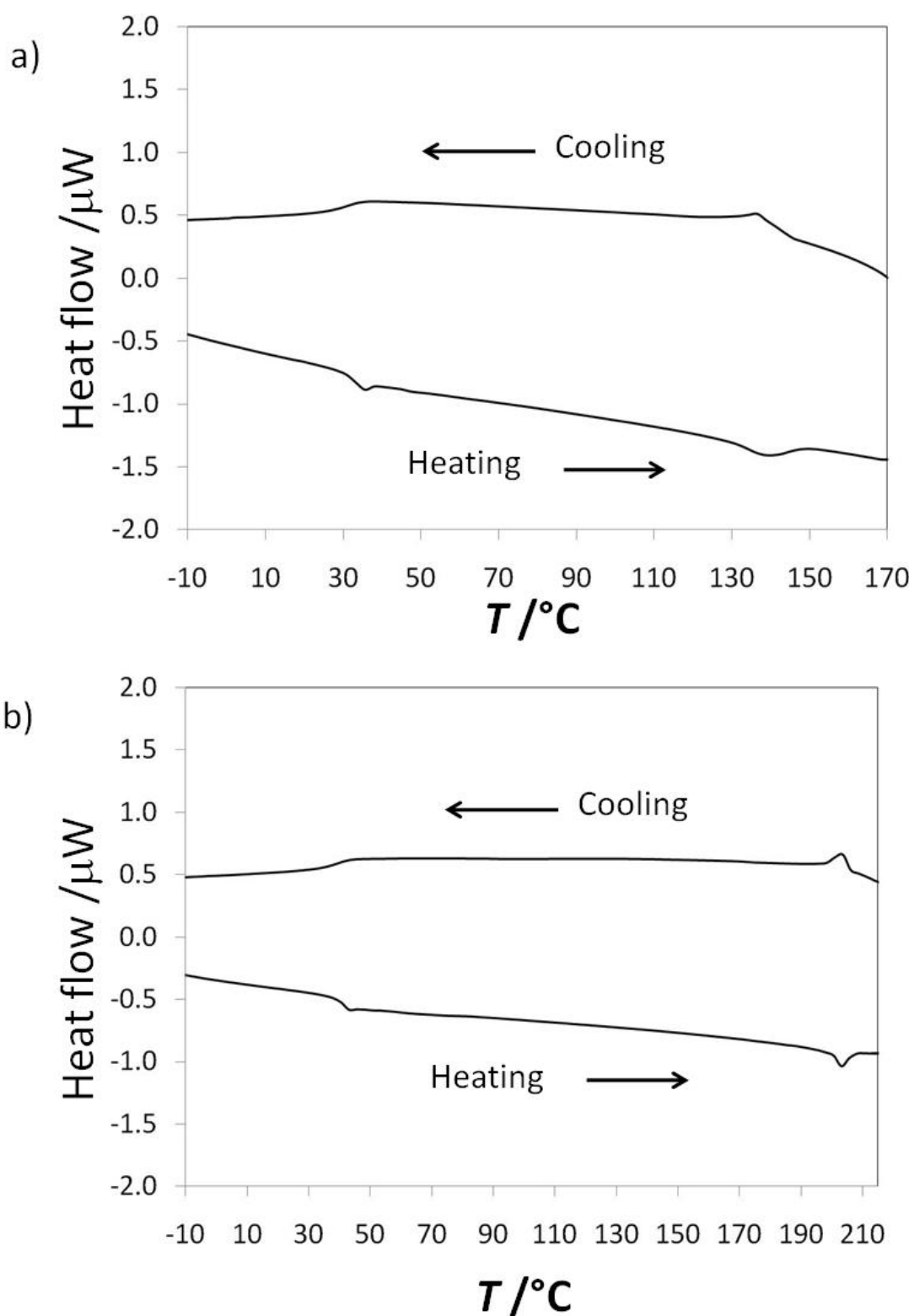


Fig. S9 (a) DSC trace of ligand L5 at 5°C/min (b) DSC trace of ligand L4 at 5°C/min.

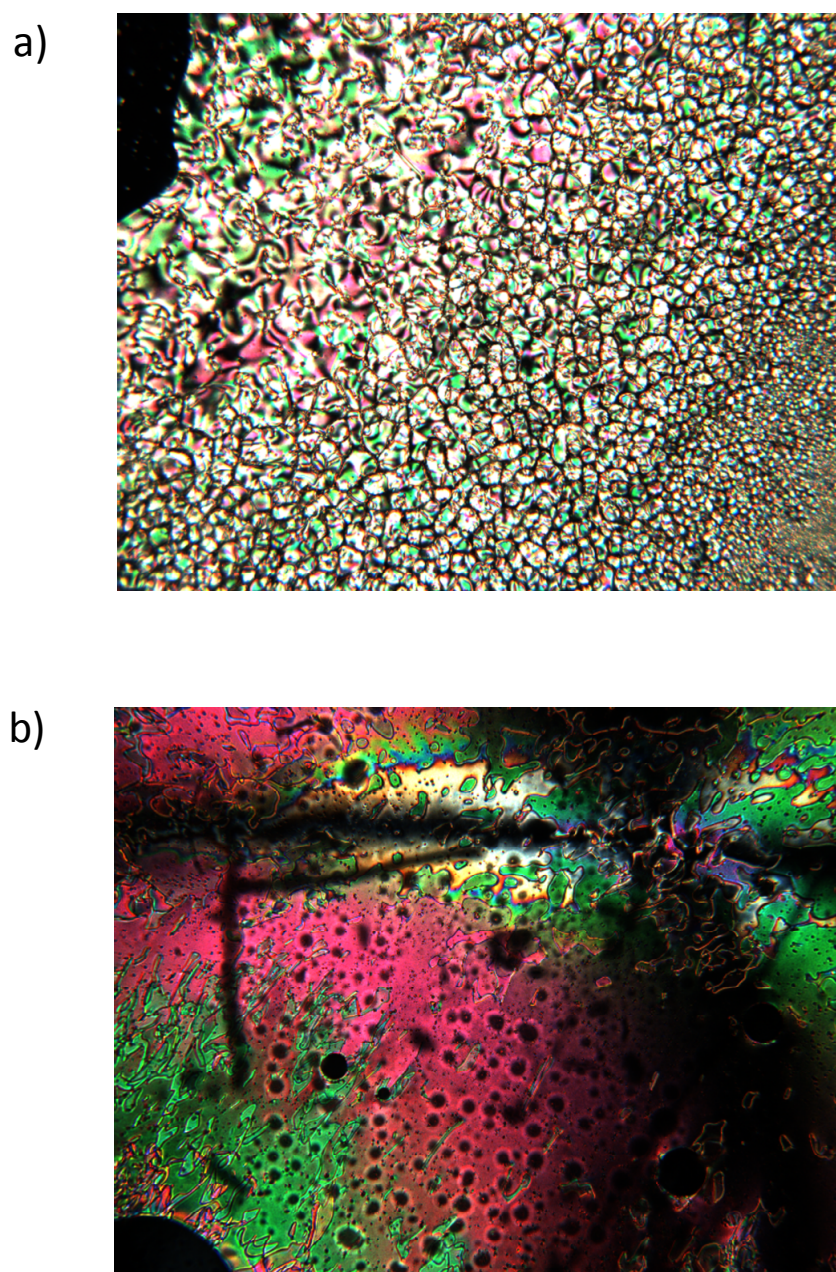


Fig. S10 (a) Optical textures observed by POM for ligand **L5** in N mesophase at 130°C after cooling from is from the isotropic liquid (b) Optical textures observed by POM for ligand **L4** in N mesophase at 140°C after cooling from is from the isotropic liquid.